Valence and Structural Transitions in the Pseudo-Ternary Germanide $Ce(Rh_{0.69}Ir_{0.31})Ge$

Etienne Gaudin and Bernard Chevalier*

Institut de Chimie de la Matière Condensée de Bordeaux (ICMCB), CNRS [UPR 9048], Université Bordeaux 1, Avenue du Docteur A. Schweitzer, 33608 Pessac Cedex, France

Birgit Heying, Ute Ch. Rodewald, and Rainer Pöttgen*

Institut für Anorganische und Analytische Chemie, Universität Münster, Corrensstrasse 36, D-48149 Münster, Germany

Received December 20, 2004. Revised Manuscript Received February 14, 2005

$Ce(Rh_{0.69}Ir_{0.31})Ge$ has been investigated by magnetization measurements, differential scanning calorimetry, and X-ray diffraction on a single crystal at 300, 150, and 100 K. For the first time, a decrease of the valence of cerium with decreasing temperature has been observed. This first-order valence transition evidenced at 236−258 K by magnetization measurements is correlated to the occurrence of a structural transition appearing between 300 and 150 K. The structural properties versus temperature of $Ce(Rh_{0.69}Ir_{0.31})Ge$ are discussed in relation to those determined on single crystals on the antiferromagnet CeRhGe and on the intermediate valence compound CeIrGe. The structure refinements revealed significantly different distortions for the [RhGe] and [IrGe] polyanionic networks, which are a direct consequence of the different electron densities at the rhodium and iridium sites, respectively. The crystal chemical peculiarities of the CeRhGe, $Ce(Rh_{0.69}Ir_{0.31})Ge$, and CeIrGe structures are discussed.

I. Introduction

Few compounds based on cerium exhibit a temperature- or pressure-induced first-order valence transition. For instance, the pseudo-ternary stannide $Ce(Ni_{0.65}Co_{0.35})Sn$ presents this transition near 50 K; its magnetic susceptibility shows a sharp drop with increasing temperature and a large thermal hysteresis between 30 and 70 K.[1] This behavior associated with a small change of the unit cell volume ($\Delta V/V = -0.003$) was explained considering a large change in the Kondo temperature T_K. Two other compounds, $Ce_{0.74}Th_{0.26}$ and CeNi, exhibit a similar valence transition.[2,3] This behavior is induced as a function of temperature (∼150 K) at ambient pressure in $Ce_{0.74}Th_{0.26}$ and as the pressure rises 3 kbar at around 100 K in CeNi. For these three compounds, the Kondo temperature of the low temperature form is higher than that determined for the high temperature form.

Previously, we have reported on an interesting transition from an antiferromagnetic behavior to an intermediate valence state in the $Ce(Rh_{1-x}Ir_x)Ge$ system.[4,5] The investigation of the compounds for $0.28 \leq x \leq 0.36$ by magnetization and electrical resistivity measurements and Ce L_{III}-edge X-ray absorption spectroscopy revealed unusual behavior: (i) their reciprocal magnetic susceptibility, measured with increasing temperature, shows a strong increase around 280, 190, and 160 K for $x = 0.28$, 0.31, and 0.33, respectively; (ii) for these compositions a very strong increase of their electrical resistivity appears when the temperature is lowered from 290 K; (iii) finally, an analysis of the Ce L_{III} absorption edge performed on $Ce(Rh_{0.72}Ir_{0.28})Ge$, has allowed determination of the average valence (υ) of cerium versus temperature: $\upsilon = 3.12$ and 3.08 for 300 and 77 K, respectively. All these results suggest that the $Ce(Rh_{1-x}Ir_x)Ge$ system presents for $0.28 \leq x \leq 0.36$ a temperature-induced first-order valence transition. In contrast to that observed for $Ce(Ni_{0.65}Co_{0.35})Sn$ or $Ce_{0.74}Th_{0.26}$, the valence transition involved in the $Ce(Rh_{1-x}Ir_x)Ge$ system induces a decrease of the valence of cerium with decreasing temperature. This transition, observed for the first time, is unique.

To characterize the valence phase transition appearing in the $Ce(Rh_{1-x}Ir_x)Ge$ system, we have investigated $Ce(Rh_{0.69}Ir_{0.31})Ge$ annealed for long time (2 months), by magnetization measurements, differential scanning calorimetry (DSC), and X-ray diffraction on a single crystal at various temperatures. We show that the temperature-induced first-order valence transition evidenced in this pseudo-ternary germanide can be correlated to the crystallographic properties.

Also, we discuss the structural properties of $Ce(Rh_{0.69}Ir_{0.31})Ge$ in relation to those of CeRhGe and CeIrGe investigated in detail via single-crystal X-ray data in order to study the influence of the cerium valence on the three-dimensional [RhGe], [$Rh_{0.69}Ir_{0.31}Ge$], and [IrGe] networks. The first characterization of CeRhGe and CeIrGe was

* Corresponding authors. E-mail: chevalie@icmcb.u-bordeaux1.fr; pottgen@uni-muenster.de.

(1) Adroja, D. T.; Echizen, Y.; Takabatake, T.; Matsumoto, Y.; Suzuki, T.; Fujita, T.; Rainford, B. D. *J. Phys.: Condens. Matter* **1999**, *11*, 543.
(2) Shapiro, S. M.; Axe, J. D.; Birgeneau, R. J.; Lawrence, J. M.; Parks, R. D. *Phys. Rev. B* **1977**, *16*, 2225.
(3) Gignoux, D.; Voiron, J. *Phys. Rev. B* **1985**, *32*, 4822.
(4) Chevalier, B.; Rogl, P.; Etourneau, J.; Besnus, M. J. *J. Magn. Magn. Mater*. **1990**, *83*, 303.
(5) Chevalier, B.; Rogl, P.; Hlil, E. K.; Tuilier, M. H.; Dordor, P.; Etourneau, J. *Z. Phys. B − Condens. Matter* **1991**, *84*, 205.

10.1021/cm040203c CCC: $30.25
Published on Web 04/13/2005

Table 1. Lattice Parameters of the Germanides CeRhGe, Ce($Rh_{0.69}Ir_{0.31}$)Ge, and CeIrGe, Space Group *Pnma*, at Different Temperatures

compound	temp/K	*a*/pm	*b*/pm	*c*/pm	*V*/nm^3	reference
CeRhGe	300	742.9(2)	446.7(2)	712.1(2)	0.2363	this work
CeRhGe	300	742.4(2)	446.8(2)	712.0(3)	0.2362	6
CeRhGe	300	742.96(39)	446.61(22)	711.97(42)	0.2362	5
CeRhGe	1.7	744.3(4)	445.4(2)	704.1(5)	0.2334	12
CeRhGe	15.7	745.6(4)	446.0(2)	704.8(4)	0.2344	12
Ce($Rh_{0.69}Ir_{0.31}$)Ge	300	711.1(45)	441.63(12)	750.65(38)	0.2358	5
Ce($Rh_{0.69}Ir_{0.31}$)Ge[a]	300	711.1(2)	441.68(7)	749.2(2)	0.2353	this work
Ce($Rh_{0.69}Ir_{0.31}$)Ge[a]	150	742.7(8)	443.6(3)	710.1(8)	0.2340	this work
Ce($Rh_{0.69}Ir_{0.31}$)Ge[a]	100	743.2(3)	444.0(6)	708.7(7)	0.2339	this work
CeIrGe	300	707.2(1)	437.42(7)	757.3(1)	0.2343	this work
CeIrGe	300	707.1(1)	437.5(1)	757.4(1)	0.2343	6
CeIrGe	300	707.30(27)	437.40(4)	757.48(18)	0.2343	5

[a] Determined from single-crystal investigation.

performed by Hovestreydt et al.[6] They investigated these ternary germanides by X-ray powder diffraction and they assigned the orthorhombic TiNiSi type (space group *Pnma*)[7] which can be considered as strong orthorhombically distorted, ordered variants of the hexagonal AlB_2 type.[8] Although rhodium and iridium have almost similar metallic and covalent radii,[9] there are distinct differences in the lattice parameters: $a = 742.4(2)$, $b = 446.8(2)$, $c = 712.0(3)$ pm for CeRhGe and $a = 707.1(1)$, $b = 437.5(1)$, $c = 757.4(1)$ pm for CeIrGe.[6] This is a direct consequence of the different valence state of cerium in both ternary germanides; Ce exhibits a trivalent state in CeRhGe and an intermediate valence state in CeIrGe.[5,10]

II. Experimental Details

A. Synthesis. A polycrystalline Ce($Rh_{0.69}Ir_{0.31}$)Ge sample was synthesized by arc-melting a stoichiometric mixture of pure elements (purity above 99.9%) in a high-purity argon atmosphere. Then, the sample was turned over and remelted several times to ensure homogeneity. The weight loss during the arc-melting process was less than 0.5 wt %. Annealing was done for two months at 1073 K by enclosing the samples in evacuated quartz tubes. No attack of the quartz tube by the sample or vice versa was observed. Characterization by electron microprobe analysis revealed a perfect chemical homogeneity. The CeRhGe and CeIrGe samples were prepared by induction levitation melting of CeGe master alloys with compacted pellets of rhodium and iridium powder as described previously.[10]

B. DSC and Magnetic Measurements. The characterization of Ce($Rh_{0.69}Ir_{0.31}$)Ge by differential scanning calorimetry was performed using a Perkin-Elmer Pyris Diamond DSC calorimeter at a cooling or heating rate of 5 K/min. The specimen for DSC was a pellet contained in an aluminum crucible maintained under protective helium gas.

Magnetization measurements were performed using a superconducting quantum interference device (SQUID) magnetometer in the temperature range 1.8−360 K and applied fields up to 5 T.

C. X-ray Diffraction Measurements. X-ray powder diffraction (Cu $K\alpha_1$ radiation) confirms that Ce($Rh_{0.69}Ir_{0.31}$)Ge crystallizes in the orthorhombic TiNiSi-type structure (space group *Pnma*) with unit cell parameters $a = 711.14(5)$, $b = 441.64(3)$, and $c = 749.59(5)$ pm in agreement with those reported previously (Table 1).[5] The polycrystalline CeRhGe and CeIrGe samples, prepared as previously described,[10] were characterized through Guinier powder patterns (imaging plate technique, Fujifilm BAS-1800) with Cu $K\alpha_1$ radiation and α-quartz ($a = 491.30$, $c = 540.46$ pm) as an internal standard. The lattice parameters (Table 1) were obtained from least-squares fits of the Guinier data. The correct indexing was ensured through intensity calculations[11] using the positional parameters of the structure refinements. The lattice parameters of the powders and the single crystals agreed well (Table 1). They are in good accordance with the literature data.

Table 2. Crystal Data and Structure Refinement for CeRhGe and CeIrGe with TiNiSi Type Structure, Space Group *Pnma*, $Z = 4$

empirical formula	CeRhGe	CeIrGe
molar mass	315.62 g/mol	404.91 g/mol
unit cell dimensions	Table 1	Table 1
calculated density	8.87 g/cm^3	11.48 g/cm^3
cryst size	20 × 30 × 70 μm^3	20 × 30 × 40 μm^3
diffractometer	Stoe IPDS-II	
detector distance	60 mm	60 mm
exposure time	12 min	11 min
ω range; increment	0−180°; 1.0°	0−180°; 1.0°
integr. param. A, B, EMS	14.0; 4.0; 0.012	14.5; 4.5; 0.012
abs coeff	38.0 mm^{-1}	88.1 mm^{-1}
transm. ratio (max/min)	2.18	2.34
F(000)	540	668
θ range	3° to 35°	3° to 35°
range in *hkl*	±11, ±6, ±11	±11, ±6, ±12
total no. reflns	3336	3284
independent reflns	562 ($R_{int} = 0.0476$)	552 ($R_{int} = 0.0253$)
reflns with $I > 2\sigma(I)$	529 ($R_\sigma = 0.0233$)	538 ($R_\sigma = 0.0126$)
data/params	562/20	552/20
GOF on F^2	1.133	1.250
final R indices [$I > 2\sigma(I)$]	R1 = 0.0311	R1 = 0.0167
	wR2 = 0.0801	wR2 = 0.0341
R indices (all data)	R1 = 0.0329	R1 = 0.0177
	wR2 = 0.0806	wR2 = 0.0343
extinction coeff	0.005(1)	0.0073(3)
largest diff. peak and hole	2.20/−2.64 e/Å^3	1.58/−1.84 e/Å^3

The refinement of the crystal structure of the Ce($Rh_{0.69}Ir_{0.31}$)Ge structure was performed at three temperatures, 300, 150, and 100 K, using a tiny single-crystal isolated from the sample by mechanical fragmentation. The data collection was carried out on an Enraf-Nonius Kappa CCD diffractometer using Mo Kα radiation. Data processing was performed with Jana 2000 software.[13] A Gaussian-type absorption correction was applied and the shape was estimated with the video microscope of the Kappa CCD.

(6) Hovestreydt, E.; Engel, N.; Klepp, K.; Chabot, B.; Parthé, E. *J. Less-Common Met.* **1982**, *85*, 247.
(7) Shoemaker, C. B.; Shoemaker, D. P. *Acta Crystallogr.* **1965**, *18*, 900.
(8) Hoffmann, R.-D.; Pöttgen, R. *Z. Kristallogr.* **2001**, *216*, 127.
(9) Emsley, J. *The Elements*; Oxford University Press: Oxford, 1999.
(10) Rogl, P.; Chevalier, B.; Besnus, M. J.; Etourneau, J. *J. Magn. Magn. Mater.* **1989**, *80*, 305.
(11) Yvon, K.; Jeitschko, W.; Parthé, E. *J. Appl. Crystallogr.* **1977**, *10*, 73.
(12) Bazela, W.; Zygmunt, A.; Szytula, A.; Ressouche, E.; Leciejewicz, J.; Sikora, W. *J. Alloys Compd.* **1996**, *243*, 106.
(13) Petricek, V.; Dusek, M. *The Crystallographic Computing System Jana 2000*; Institute of Physics: Praha, Czech Republic, 2000.

Table 3. Crystal Data and Structure Refinement for $Ce(Rh_{0.69}Ir_{0.31})Ge$ at 300, 150, and 100 K with TiNiSi Type Structure, Space Group *Pnma*, $Z = 4$

empirical formula		$Ce(Rh_{0.69}Ir_{0.31})Ge$	
molar mass		343.30 g/mol	
temperature	300 K	150 K	100 K
unit cell dimensions		Table 1	
calcd density (g/cm^3)	9.69	9.74	9.75
crystl size (300 K)		$58 \times 16 \times 14\ \mu m^3$	
diffractometer		Enraf-Nonius KappaCCD	
detector distance		32 mm	
exposure time	20 s	40 s	40 s
scan		phi-scan + ω-scan	
abs coeff		53.85 mm^{-1}	
transm coeff, T_{min}/T_{max}	0.201/0.509	0.179/0.651	0.236/0.681
F(000)		580	
θ range		3° to 35°	
range in *hkl*	±11, ±7, ±11	±11, ±7, ±11	±11, ±7, ±11
total no. reflns	5709	5328	5730
independent reflns	568 ($R_{int} = 0.1493$)	557 ($R_{int} = 0.0984$)	559 ($R_{int} = 0.1154$)
reflns with $I > 3\sigma(I)$	311 ($R_\sigma = 0.0996$)	399 ($R_\sigma = 0.1176$)	411 ($R_\sigma = 0.0993$)
data/param	568/18	557/18	559/19
GOF on F^2	1.11	1.39	1.33
Final R indices [$I > 3\sigma(I)$]	R1 = 0.0372	R1 = 0.0371	R1 = 0.0347
	wR2 = 0.0757	wR2 = 0.0823	wR2 = 0.0717
R indices (all data)	R1 = 0.1043	R1 = 0.0788	R1 = 0.0745
	wR2 = 0.0939	wR2 = 0.0960	wR2 = 0.0866
Largest diff. peak and hole	2.33/−1.40 e/Å^3	2.51/−2.12 e/Å^3	2.26/−2.41 eÅ^3

Irregularly shaped single crystals of CeRhGe and CeIrGe were selected from the crushed polycrystalline samples and first examined on Buerger precession cameras (white Mo radiation, Fujifilm BAS-1800 imaging plate system) to check the quality for intensity data collection. The data sets for the two crystals were collected at room temperature by use of a Stoe IPDS-II diffractometer (oscillation mode) with graphite monochromatized Mo Kα radiation (71.073 pm). Numerical absorption corrections were applied to the data.

D. Structures Determination. The isotypy of CeRhGe and CeIrGe with TiNiSi was already evident from the earlier X-ray powder investigations. The systematic extinctions were compatible with space group *Pnma*. During the integration process, both data sets were carefully investigated for potential superstructure reflections, since the related germanides CePdGe[14] and CePtGe[15] showed tripling and doubling of the unit cells due to different colorings in the T−Ge ordering (T = transition metal). For CeRhGe and CeIrGe no hints of cell enlargements were evident. The starting atomic parameters were deduced from automatic interpretations of direct methods with SHELXS-97[16] and both structures were refined with SHELXL-97 (full-matrix least-squares on F^2)[17] with anisotropic displacement parameters for all atoms. The occupancy parameters were refined in a separate series of least-squares cycles to check for deviations from the ideal composition. Since all sites were fully occupied within two standard deviations, the ideal occupancies were assumed again in the last cycles. The final difference Fourier syntheses were flat for both data sets (Table 2). The positional parameters and interatomic distances of the refinements are listed in Tables 4 and 5. Further data on the structure refinements are available.[18] The present structure refinement of CeRhGe is considerably more precise than a previous neutron powder diffraction study at 1.7 and 15.7 K.[12]

Table 4. Atomic Coordinates and Isotropic Displacement Parameters (pm^2) of CeRhGe, $Ce(Rh_{0.69}Ir_{0.31})Ge$, and CeIrGe[a]

atom	occ.	*x*	*y*	*z*	U_{eq}[b]
		CeRhGe (300 K data)			
Ce	1.0	−0.01535(6)	1/4	0.67480(7)	112(2)
Rh	1.0	0.63935(8)	1/4	0.4298(1)	118(2)
Ge	1.0	0.3037(1)	1/4	0.3905(1)	108(2)
		$Ce(Rh_{0.69}Ir_{0.31})Ge$ (100 K data)			
Ce	1.0	−0.01520(9)	1/4	0.67168(10)	55(2)
Rh	0.69	0.637(2)	1/4	0.432(2)	56(2)
Ir	0.31	0.639(2)	1/4	0.428(2)	56[c]
Ge	1.0	0.3040(2)	1/4	0.3885(2)	55(3)
		$Ce(Rh_{0.69}Ir_{0.31})Ge$ (150 K data)			
Ce	1.0	−0.01468(10)	1/4	0.67239(11)	68(2)
Rh	0.69	0.6348(9)	1/4	0.4326(10)	65(3)
Ir	0.31	0.6429(10)	1/4	0.4275(12)	65[c]
Ge	1.0	0.3040(2)	1/4	0.3893(3)	62(4)
		$Ce(Rh_{0.69}Ir_{0.31})Ge$ (300 K data)			
Ce	1.0	−0.01369(11)	1/4	0.69844(11)	108(2)
Rh	0.69	0.6901(4)	1/4	0.4132(5)	97(3)
Ir	0.31	0.7155(4)	1/4	0.4125(5)	97[c]
Ge	1.0	0.3157(2)	1/4	0.4143(2)	117(4)
		CeIrGe (300 K data)			
Ce	1.0	−0.01105(4)	1/4	0.69917(4)	83(1)
Ir	1.0	0.70834(3)	1/4	0.41068(3)	92(1)
Ge	1.0	0.31949(9)	1/4	0.41591(8)	88(1)

[a] All atoms lie on the Wyckoff site 4c (*x*, 1/4, *z*). [b] U_{eq} is defined as one-third of the trace of the orthogonalized U_{ij} tensor. [c] These displacement parameters were constrained to those of the Rh positions.

The three crystallographic structures of $Ce(Rh_{0.69}Ir_{0.31})Ge$ at 300, 150, and 100 K have been solved in the *Pnma* space group with the JANA 2000 program.[13] The starting positions have been deduced from direct method (SHELXS-97[16]) and correspond to those obtained for CeIrGe and CeRhGe. The main difference is the splitting of the Ir/Rh position, with the two atoms being localized in very close but different crystallographic positions. The occupancy ratio of Rh and Ir position has been fixed to 0.69 and 0.31, respectively. To avoid strong correlations, the same isotropic atomic displacement parameter (ADP) has been used for both positions. Anisotropic ADP has been used for the other positions. All classical refinement validation criteria are given in Table 3. The atomic positions and interatomic distances are given in Tables 4 and 5.

(14) Niepmann, D.; Prots', Yu. M.; Pöttgen, R.; Jeitschko, W. *J. Solid State Chem.* **2000**, *154*, 329.
(15) Prots', Yu. M.; Pöttgen, R.; Niepmann, D.; Wolff, M. W.; Jeitschko, W. *J. Solid State Chem.* **1999**, *142*, 400.
(16) Sheldrick, G. M. *SHELXS-97, Program for the Solution of Crystal Structures*; University of Göttingen: Germany, 1997.
(17) Sheldrick, G. M. *SHELXL-97, Program for Crystal Structure Refinement*; University of Göttingen: Germany, 1997.
(18) Details may be obtained from: Fachinformationszentrum Karlsruhe, D-76344 Eggenstein-Leopoldshafen, Germany, by quoting the Registry Nos. CSD-414508 (CeRhGe) and CSD-414509 (CeIrGe).

Table 5. Interatomic Distances (pm) of the Orthorhombic Compounds CeRhGe and $CeRh_{0.69}Ir_{0.31}Ge$ at 300, 150, and 100 K, and CeIrGe[a]

CeRhGe[b] (300 K)				$Ce(Rh_{0.69}Ir_{0.31})Ge$ (300 K)				$Ce(Rh_{0.69}Ir_{0.31})Ge$ (150 K)				$Ce(Rh_{0.69}Ir_{0.31})Ge$ (100 K)				CeIrGe[b] (300 K)			
Ce:	2	Rh	302.2	Ce:	1	Ir	288.0	Ce:	1	Rh	301.4	Ce:	2	Ir	301.2	Ce:	1	Ir	295.2
	1	Rh	304.1		1	Rh	300.0		2	Rh	302.3		2	Rh	302.5		2	Ir	304.9
	1	Rh	310.2		2	Rh	300.7		2	Ir	302.0		1	Rh	302.8		2	Ge	305.2
	1	Ge	311.7		2	Ge	307.9		1	Ir	307.0		1	Ir	306.0		1	Ge	315.2
	2	Ge	312.9		2	Ir	308.4		1	Ir	307.8		1	Rh	309.3		2	Ir	317.1
	2	Ge	313.4		1	Ge	314.4		1	Ge	310.6		1	Ir	309.6		1	Ge	317.3
	2	Ce	335.2		1	Ge	316.5		1	Rh	311.0		1	Ge	310.8		2	Ge	321.0
	1	Ge	337.5		2	Ir	317.2		2	Ge	311.9		2	Ge	311.7		1	Ir	333.7
	2	Rh	365.3		2	Ge	319.4		2	Ge	312.1		2	Ge	312.3		2	Ce	361.9
	2	Ce	386.6		1	Rh	325.1		2	Ce	331.1		2	Ce	330.2		2	Ce	372.9
					2	Rh	329.7		1	Ge	339.1		1	Ge	339.4				
					1	Ir	334.0		2	Ir	361.2		2	Ir	363.9				
					2	Ce	363.9		2	Rh	366.6		2	Rh	365.6				
					2	Ce	370.9		2	Ce	387.4		2	Ce	387.8				
				Ir:	1	Rh	18.1	Ir:	1	Rh	7.0	Ir:	1	Rh	3.0	Ir:			
					1	Ge	255.1		1	Ge	253.3		1	Ge	250.5		2	Ge	255.9
					2	Ge	257.1		1	Ge	255.1		1	Ge	255.6		1	Ge	259.5
					1	Ge	284.3		2	Ge	260.0		2	Ge	260.8		1	Ge	275.0
					1	Ce	288.0		2	Ce	302.0		2	Ce	301.2		1	Ce	295.2
					2	Ce	308.4		1	Ce	307.0		1	Ce	306.0		2	Ce	304.9
					2	Ce	317.2		1	Ce	307.8		1	Ce	309.6		2	Ce	317.1
					1	Ce	334.0		2	Rh	318.6		2	Rh	318.1		1	Ce	333.7
					2	Rh	386.0		2	Ir	323.7		2	Ir	320.0		2	Ir	391.1
					2	Ir	399.9		2	Ce	361.2		2	Ce	363.9				
Rh:				Rh:	1	Ir	18.1	Rh:	1	Ir	7.0	Rh:	1	Ir	3.0				
	1	Ge	250.9		2	Ge	255.9		1	Ge	247.6		1	Ge	249.4				
	1	Ge	258.7		1	Ge	261.2		2	Ge	259.2		1	Ge	258.9				
	2	Ge	260.9		1	Ge	266.2		1	Ge	261.1		2	Ge	259.6				
	2	Ce	302.2		1	Ce	300.0		1	Ce	301.4		2	Ce	302.5				
	1	Ce	304.1		2	Ce	300.7		2	Ce	302.3		1	Ce	302.8				
	1	Ce	310.2		1	Ce	325.1		1	Ce	310.9		1	Ce	309.3				
	2	Rh	320.6		2	Ce	329.7		2	Rh	313.6		2	Rh	316.3				
	2	Ce	365.3		2	Rh	372.5		2	Ir	318.6		2	Ir	318.1				
					2	Ir	386.0		2	Ce	366.6		2	Ce	365.6				
Ge:	1	Rh	250.9	Ge:	1	Ir	255.1	Ge:	1	Rh	247.6	Ge:	1	Rh	249.4	Ge:	2	Ir	255.9
	1	Rh	258.7		2	Rh	255.9		1	Ir	253.3		1	Ir	250.5		1	Ir	259.5
	2	Rh	260.9		2	Ir	257.1		1	Ir	255.1		1	Ir	255.6		1	Ir	275.0
	1	Ce	311.7		1	Rh	261.0		2	Rh	259.2		1	Rh	258.9		2	Ce	305.2
	2	Ce	312.9		1	Rh	266.2		2	Ir	260.0		2	Rh	259.6		1	Ce	315.2
	2	Ce	313.4		1	Ir	284.3		1	Rh	261.1		2	Ir	260.8		1	Ce	317.3
	1	Ce	337.5		2	Ce	307.9		1	Ce	310.6		1	Ce	310.8		2	Ce	321.0
	2	Ge	399.1		2	Ce	314.4		2	Ce	311.9		2	Ce	311.7		2	Ge	359.5
					1	Ce	316.5		2	Ce	312.1		2	Ce	312.3				
					1	Ce	319.4		1	Ce	339.1		1	Ce	339.4				
					2	Ge	366.0		2	Ge	398.3		2	Ge	398.9				

[a] Standard deviations are all less than 1 pm, except for Rh−Ir distances (2 pm). All distances within the first coordination spheres are listed. Note that the rhodium and iridium positions in $Ce(Rh_{0.69}Ir_{0.31})Ge$ are only occupied by 69 and 31%, respectively. [b] Distances calculated with powder lattice parameters.

III. Results and Discussion

A. Magnetic Properties of $Ce(Rh_{0.69}Ir_{0.31})Ge$. Figure 1 shows the temperature dependence of the reciprocal magnetic susceptibility χ_m^{-1} of $Ce(Rh_{0.69}Ir_{0.31})Ge$ measured with increasing temperature from 1.8 to 360 K then with decreasing temperature. Three characteristics can be distinguished from the curve $\chi_m^{-1} = f(T)$ relative to the heating process: (i) between 50 and 200 K, the curve follows a Curie−Weiss law with the effective magnetic moment $\mu_{eff} = 1.91(3)\ \mu_B$/mol and the paramagnetic Curie temperature $\theta_p = -39(2)$ K; (ii) then χ_m^{-1} increases sharply between 225 and 300 K; in this range a transition temperature $T_{t1} = 258(2)$ K can be defined as the occurrence of a maximum in the derivative curve $d\chi_m^{-1}/dT = f(T)$; (iii) finally, above 300 K, χ_m^{-1} is practically independent of the temperature, taking a constant value of 1045(5) mol/emu. The same characteristics are observed during the cooling process; in this case the transition temperature $T_{t2} = 236(2)$ K is determined. The sharp drop of χ_m^{-1} at T_{t1} or T_{t2} and the presence of large thermal hysteresis ($\Delta T = 22(2)$ K) indicate a first-order valence transition for cerium.

The effective paramagnetic moment ($\mu_{eff} = 1.91(3)\ \mu_B$/mol) obtained for $Ce(Rh_{0.69}Ir_{0.31})Ge$ in the temperature range 50−200 K is smaller than that calculated for a free Ce^{3+} ion (2.54 μ_B). This μ_{eff}-value agrees with the presence of 75% of Ce^{3+} ion in the compound. The analysis of the curve $\chi_m^{-1} = f(T)$ between 50 and 200 K suggests that the cerium presents two electronic configurations: the major part has a trivalent state whereas the minor part shows an intermediate valence state. We note that the percentage of trivalent cerium (75%) is nearly similar to the atomic composition in rhodium (69%). In other words, the electronic configuration of the cerium appears be influenced by its crystallographic environment. Another observation concerns the value of $\chi_m^{-1} =$ 1045(5) mol/emu above 300 K. This is comparable to those determined previously in the system $Ce(Rh_{1-x}Ir_x)Ge$ for x

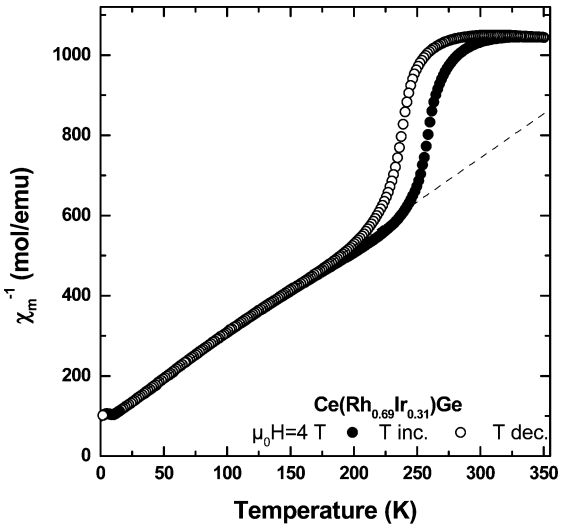

Figure 1. Temperature dependence of the reciprocal magnetic susceptibility, measured with an applied field $\mu_0 H = 4$ T, of $Ce(Rh_{0.69}Ir_{0.31})Ge$. Solid and open circles show the measurements performed with increasing and decreasing the temperature, respectively. Dashed line indicates the Curie−Weiss law determined between 50 and 200 K.

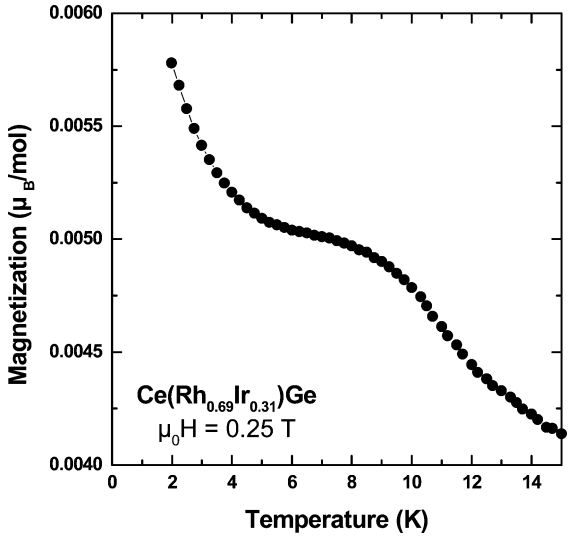

Figure 2. Temperature dependence of the magnetization of $Ce(Rh_{0.69}Ir_{0.31})Ge$ measured at the applied magnetic field $\mu_0 H = 0.25$ T.

= 0.39, 0.42, or 0.49 where the cerium exhibits an intermediate valence behavior.[5]

At low temperature, the thermal dependence of the magnetization of $Ce(Rh_{0.69}Ir_{0.31})Ge$ shows the occurrence of a shoulder near 8 K (Figure 2). Similar behavior was observed for the ternary germanide CeRhGe which orders antiferromagnetically below $T_N = 9.3$ K as evidenced by specific heat measurements[10] and neutron powder diffraction.[12] The same investigation is considered to determine the magnetic properties of $Ce(Rh_{0.69}Ir_{0.31})Ge$ at low temperature.

B. Differential Scanning Calorimetry on $Ce(Rh_{0.69}Ir_{0.31})Ge$. Figure 3 presents the DSC measurements performed below 350 K on $Ce(Rh_{0.69}Ir_{0.31})Ge$ with decreasing temperature then increasing temperature. A maximum corresponding to the first-order valence transition is observed at 228(2) K and 256(2) K, respectively, during the cooling and the heating processes. These transition temperatures determined by DSC study are in agreement with those resulting from the magnetization measurements.

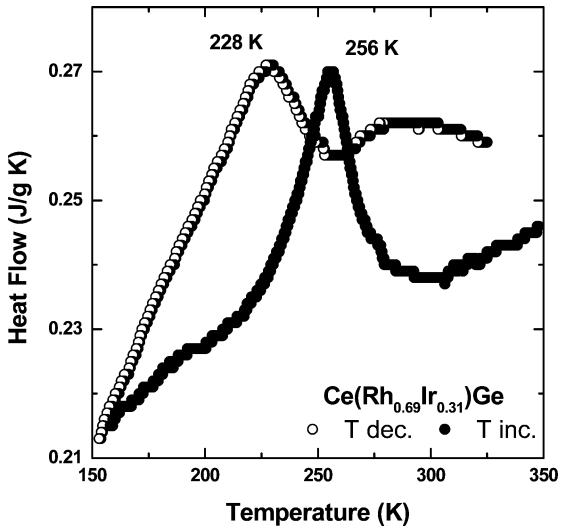

Figure 3. DSC cooling−heating curves for $Ce(Rh_{0.69}Ir_{0.31})Ge$.

C. Structural Properties of CeRhGe, $Ce(Rh_{0.69}Ir_{0.31})Ge$, and CeIrGe. To explain the first-order valence transition observed for $Ce(Rh_{0.69}Ir_{0.31})Ge$, we have investigated its crystallographic properties at three temperatures, 300, 150, and 100 K, using X-ray diffractometry on a single crystal. These properties are discussed in relation with those determined at room temperature for the first time for CeRhGe and CeIrGe.

The refinement of the $Ce(Rh_{0.69}Ir_{0.31})Ge$ structure at 100, 150, and 300 K revealed split positions for rhodium and iridium with occupancy parameters of 69 and 31%. The largest difference between these two positions occurs for the 300 K data set, resulting in a Rh−Ir split distance of 18 pm.

Our study concerning $Ce(Rh_{0.69}Ir_{0.31})Ge$ reveals that this compound undergoes a structural transition between 300 and 150 K which strongly influences its unit cell parameters (Table 1) and the atomic coordinates of the constituents (Table 4). At 300 K, the unit cell parameters of $Ce(Rh_{0.69}Ir_{0.31})Ge$ are comparable to those determined for CeIrGe where the *a* parameter is smaller than the *c* parameter. In contrast, at 150 K, the unit cell parameters of $Ce(Rh_{0.69}Ir_{0.31})Ge$ and CeRhGe exhibit strong similarities; in these cases the *a*-parameter is higher than the *c*-parameter (Table 1). This structural transition is accompanied by a small decrease of the unit cell volume ($\Delta V/V = -0.0055$).

The thermal dependence of the unit cell parameters of $Ce(Rh_{0.69}Ir_{0.31})Ge$ can be compared to that observed versus composition for the system $Ce(Rh_{1-x}Ir_x)Ge$.[5] At 300 K, two ranges of composition are distinguished: for $0.25 < x \leq 1.0$ the *a* parameter is smaller than the *c* parameter, whereas for $0.0 \leq x \leq 0.25$ the opposite is evidenced. These structural considerations are correlated to the major electronic state of cerium in the system: Ce shows principally an intermediate valence state for $0.25 < x \leq 1$ and a trivalent state for $0 \leq x \leq 0.25$. In other words, two routes exist in order to evidence a first-order valence transition of cerium in the $Ce(Rh_{1-x}Ir_x)Ge$ system: the first is observed versus composition near the critical value $x = 0.25$ and the second appears versus temperature for $Ce(Rh_{0.69}Ir_{0.31})Ge$.

The germanides studied here all crystallize with the well-known orthorhombic TiNiSi[7] type structure. The crystal

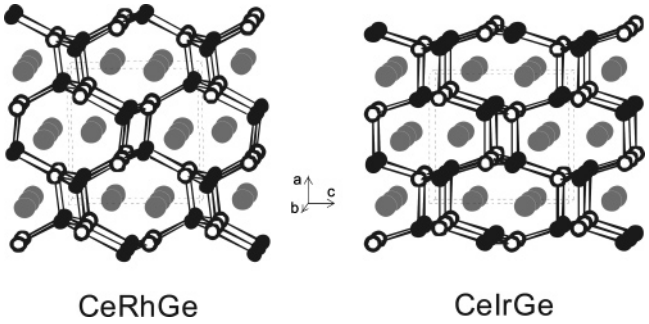

Figure 4. View of the CeRhGe and CeIrGe structures approximately along the *b* axis. Cerium, transition metal, and germanium atoms are drawn as medium gray, black filled, and open circles, respectively. The three-dimensional [TGe] networks are emphasized.

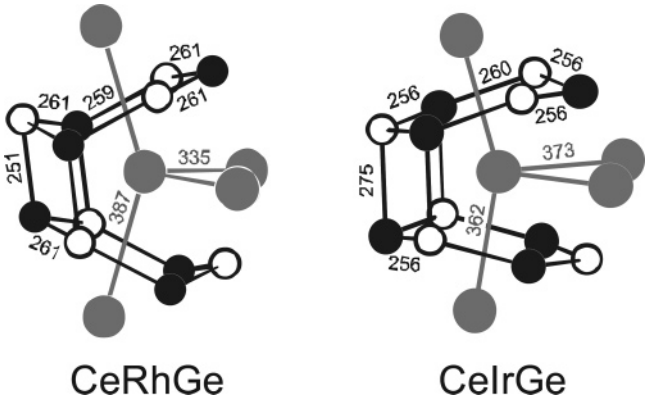

Figure 5. Coordination of the cerium atoms in CeRhGe and CeIrGe. The cerium, transition metal, and germanium atoms are drawn as medium gray, black filled, and open circles, respectively. Relevant interatomic distances are indicated in units of pm.

chemistry and chemical bonding of such intermetallics have been discussed intensively in the literature.[6,8,19−22] Here, we focus on the structural and chemical bonding peculiarities that are involved in the cerium valence change in going from CeRhGe to CeIrGe. The structural peculiarities of $Ce(Rh_{0.69}Ir_{0.31})Ge$ at 100, 150, and 300 K parallel these results; i.e., the 100 and 150 K data are similar to CeRhGe, whereas the 300 K data correspond to those of CeIrGe.

As is evident from Figure 4, the structures of CeRhGe and CeIrGe derive from the well-known aristotype AlB_2[8] with a strong orthorhombic distortion and significant puckering of the hexagonal networks. The group−subgroup scheme for symmetry reduction is given in ref 8. The transition metal and germanium atoms are well ordered on the boron positions, resulting in Rh_3Ge_3 and Ir_3Ge_3 hexagons. The latter is evident from the cerium nearest-neighbor environments presented in Figure 5. Due to the strong puckering, the [RhGe] and [IrGe] polyanionic networks in CeRhGe and CeIrGe are three-dimensional (Figure 4).

The first remarkable difference between CeRhGe and CeIrGe is evident from the X-ray powder data. The *a* lattice parameter of CeRhGe is about 35 pm larger than that of CeIrGe, whereas the *c* lattice parameter of CeRhGe is about 45 pm smaller (Table 1). The cell volume is almost the same. This anisotropy in the lattice parameters is a direct consequence of the different cerium valence in CeRhGe and CeIrGe and furthermore significantly influences the puckering of the Rh_3Ge_3 and Ir_3Ge_3 hexagons.

The near-neighbor environment of the cerium atoms in both structures is presented in Figure 5. Each cerium atom in CeRhGe and CeIrGe has 16 nearest neighbors, four cerium, six transition metal, and six germanium atoms, however, with considerably different interatomic distances. Although rhodium (125 pm) and iridium (126 pm) have similar covalent radii,[9] the average Ce−Ir distance of 312 pm is much shorter than the average Ce−Rh distance of 324 pm. In parallel, also the average Ce−Ge distance is smaller in the iridium compound (314 vs 317 pm). The longer Ce−Rh distances might be indicative for stronger Ce−T bonding in CeIrGe as compared to CeRhGe.

Within the three-dimensional [RhGe] and [IrGe] polyanions, each transition metal atom T has a strongly distorted tetrahedral germanium coordination at T−Ge distances ranging from 251 to 261 pm (CeRhGe, average 258 pm) and from 256 to 275 pm (CeIrGe, average 262 pm). All of these T−Ge distances are slightly longer than the sums of the covalent radii of 247 pm for Rh+Ge and 248 pm for Ir+Ge.[9] The T−Ge bonding thus does not play the predominant role in CeRhGe and CeIrGe. In other ternary germanides with similar $IrGe_4$ units within the polyanionic network the Ir−Ge distances are shorter, e.g., 247−268 pm in Yb_2IrGe_2, 251−258 pm in LuIrGe, or 246−264 pm in $Lu_3Ir_2Ge_3$.[23] The same holds for other rhodium-based germanides.

A striking difference occurs for the Ce−Ce distances in CeRhGe (335 and 387 pm) and CeIrGe (362 and 373 pm). The shorter Ce−Ce distances in CeRhGe are even shorter than in *fcc* cerium (365 pm)[24] and also below the Hill limit for 4*f* electron localization.[25] Now, together with $CePt_2$, CeRhGe seems to be the second exception from the Hill rule.

The variation of the Ce−Ce distances seems to be a consequence of the different tilts of the Rh_3Ge_3 and Ir_3Ge_3 hexagons. In CeRhGe the tilt is more pronounced and the cerium coordination sphere is more open (right-hand part of the polyhedron in Figure 5) with respect to CeIrGe. Consequently the cerium atoms can move toward each other, leading to the short Ce−Ce contacts at 335 pm. On the other hand, the Ce−Ce distances above and below are longer (387 pm). This trend is opposite in CeIrGe.

Finally we discuss the tilt of the T_2Ge_2 parallelograms (Figures 5 and 6) that are formed due to the puckering of the hexagons. As is evident from Figures 4 and 5, these T_2Ge_2 parallelograms are condensed and form one-dimensional ladders that extend along the *b* axis. In the large family of TiNiSi related intermetallics, these T_2Ge_2 parallelograms show different tilts. Nuspl et al.[20] have investigated the chemical bonding in these intermetallics, considering the electronegativity differences between the T and X atoms and

(19) Landrum, G. A.; Hoffmann, R.; Evers, J.; Boysen, H. *Inorg. Chem.* **1998**, *37*, 5754.
(20) Nuspl, G.; Polborn, K.; Evers, J.; Landrum, G. A.; Hoffmann, R. *Inorg. Chem.* **1996**, *35*, 6922.
(21) Bojin, M. D.; Hoffmann, R. *Helv. Chim. Acta* **2003**, *86*, 1653.
(22) Bojin, M. D.; Hoffmann, R. *Helv. Chim. Acta* **2003**, *86*, 1683.
(23) Rodewald, U. Ch.; Pöttgen, R. *Solid State Sci.* **2003**, *5*, 487.
(24) Donohue, J. *The Structures of the Elements*; Wiley: New York, 1974.
(25) Hill, H. H. In *Plutonium and Other Actinides*; Miner, W. N., Ed.; Vol. 17 of the Nuclear Materials Series; American Institute of Mining, Metallurgical, and Petroleum Engineers: New York, 1970; Vol. 2.

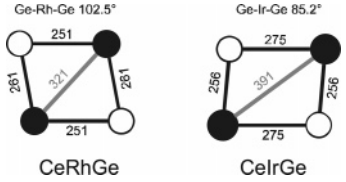

Figure 6. Comparison of the interatomic distances (pm) and bond angles (deg) in the Rh_2Ge_2 and Ir_2Ge_2 parallelograms in CeRhGe and CeIrGe. The transition metal and germanium atoms are drawn as filled and open circles, respectively. For details see text.

the valence electron concentration as well. Since CeRhGe and CeIrGe have the same electron count, we need to discuss only the electronegativity/electron density argument here. The parallelograms tilt to maximize the distance (minimize the repulsion) between the centers which show the higher electron density. In CeRhGe the Rh_2Ge_2 parallelogram is "left-tilted" leaving shorter Rh−Rh (321 pm) and longer Ge−Ge (399 pm) distances. Consequently, we find the higher electron density at the germanium centers, pointing to a true germanide character for CeRhGe. This is different in CeIrGe, where the Ir_2Ge_2 parallelogram is "right-tilted" with longer Ir−Ir (391 pm) and shorter Ge−Ge (360 pm) distances. Now we observe the higher electron density at the iridium atoms. Thus, the excess electron density that arises from the partial oxidation of Ce^{III} to Ce^{IV} in CeIrGe is localized at the iridium atoms.

In a nutshell, the TiNiSi type structure leaves different possibilities for structural distortions, accommodating different types of compounds with different physical properties. However, in view of the significantly different structural distortions, strictly speaking, CeRhGe and CeIrGe are not isotypic, but isopointal.[26,27]

The structural transition observed for $Ce(Rh_{0.69}Ir_{0.31})Ge$ modifies greatly the interatomic distances Ce−Rh or Ir. Between 300 and 150 K, the average distances Ce−Rh and Ce−Ir increase from 314 to 325 pm and from 312 to 323 pm, respectively. On the contrary, the average distance Ce−Ge is weakly affected by the structural transition; Ce−Ge changes from 313 to 316 pm. These crystallographic data suggest that the chemical bonding between cerium and rhodium or iridium plays an important role on the electronic state of cerium in the system $Ce(Rh_{1-x}Ir_x)Ge$. As previously discussed, the T_2Ge_2 parallelogram tilt has been attributed to the repulsion between the atoms with the highest electron density or electronegativity. In Figure 7 structures of $Ce(Rh_{0.61}Ir_{0.39})Ge$ at 300 and 100 K are shown and are similar to those of CeIrGe and CeRhGe, respectively, with the same T_2Ge_2 parallelogram geometry (see Figure 8). As observed in CeIrGe, in the low temperature form of $Ce(Rh_{0.61}Ir_{0.31})Ge$ the T−T distance (T = Rh/Ir) is greater than the Ge−Ge distance and can be correlated to the increase of the charge transfer from cerium to iridium and rhodium below the phase transition temperature. At 100 K the splitting between rhodium and iridium positions is very small (d_{Rh-Ir} = 3 pm). Then almost only one cerium atom's surrounding is observed with statistical distribution of rhodium and iridium atoms. In the case of $CeIr_2Si_2$ and $CeRh_2Si_2$[28,29] with

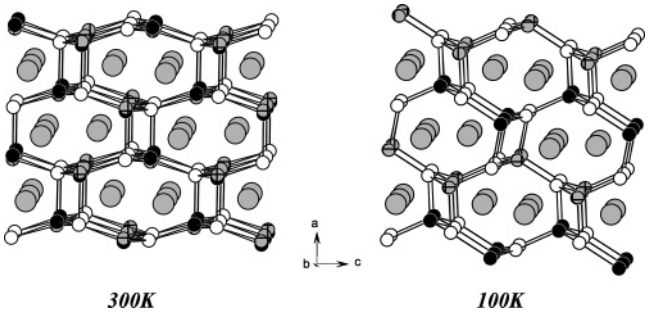

Figure 7. View of the $Ce(Rh_{0.69}Ir_{0.31})Ge$ structure at 300 and 100 K approximately along the *b* axis. Cerium, rhodium, iridium, and germanium atoms are drawn as medium gray, black filled, gray with black hatching, and open circles, respectively. The three-dimensional [(Rh, Ir)Ge] network is emphasized. For the structure at 100 K the iridium and rhodium atoms are almost at the same position with statistical occupancy distribution.

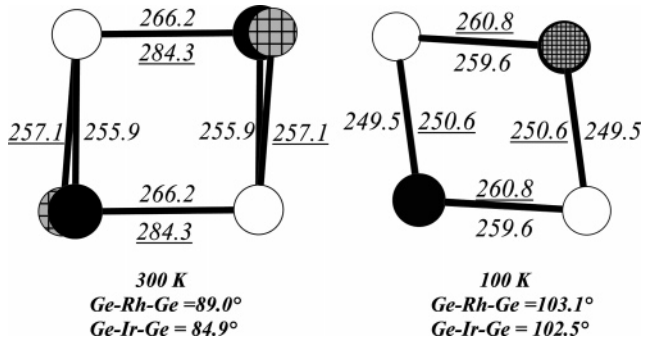

Figure 8. View of the $(Rh_{0.69}Ir_{0.31})_2Ge_2$ parallelograms in $Ce(Rh_{0.69}Ir_{0.31})$-Ge at 300 and 100 K. Rhodium, iridium, and germanium atoms are drawn as black filled, gray with black hatching, and open circles, respectively. The Ge−Ir distance (pm) values are underlined.

tetragonal $ThCr_2Si_2$ structure the valence of cerium is equal to 3.32 and 3, respectively. In both structures the Ce−Ir and Ce−Rh distances are very close, 326 and 325 pm, and correspond to those observed for the low temperature form of the title compound (Table 5). This means that the charge transfer between cerium and the transition metal for the same distance is higher in the case of iridium and this can be attributed to the more diffuse character of the 5*d* orbitals compare to the 4*d* orbitals of rhodium. This higher electron transfer in the case of iridium explains that 25% of cerium with intermediate valence is still observed at low temperature.

IV. Conclusion

Magnetization measurements show that the germanide $Ce(Rh_{0.69}Ir_{0.31})Ge$ presents in the temperature range 236−258 K a first-order valence transition with cerium being in an intermediate valent state over the whole temperature range, with essentially trivalent cerium below 200 K and an essentially tetravalent valence state above 300 K. This transition constitutes the first example among cerium intermetallics; its valence increases with the temperature.

The first-order valence transition of $Ce(Rh_{0.69}Ir_{0.31})Ge$ is correlated to a structural transition evidenced by X-ray diffraction on a single crystal at 300, 150, and 100 K. At 300 K, the structural properties of $Ce(Rh_{0.69}Ir_{0.31})Ge$ are

(26) Gelato, L. M.; Parthé, E. *J. Appl. Crystallogr.* **1987**, *20*, 139.
(27) Parthé, E.; Gelato, L. M. *Acta Crystallogr.* **1984**, *40A*, 169.
(28) Buffat, B.; Chevalier, B.; Tuilier, M. H.; Lloret, B.; Etourneau, J. *Solid State Commun.* **1986**, *59*, 17.
(29) Quezel, S.; Rossat-Mignod, J.; Chevalier, B.; Lejay, P.; Etourneau, J. *Solid State Commun.* **1984**, *49*, 685.

similar to that observed for the intermediate valence compound CeIrGe, whereas at 150 and 100 K a resemblance exists between $Ce(Rh_{0.69}Ir_{0.31})Ge$ and the antiferromagnetic germanide CeRhGe. The magnetic properties of the $Ce(Rh_{1-x}Ir_x)Ge$ system are governed by the strength of the chemical bonding Ce−Rh or Ce−Ir. This change in chemical bonding is directly connected to the tilt of the T_2Ge_2 parallelogram and then to the inversion of the *c*/*a* ratio.

Acknowledgment. We thank D. Denux for his assistance during the DSC measurements. This work was supported by the Deutsche Forschungsgemeinschaft.

CM040203C